Intermolecular effects in the center-of-mass dynamics of unentangled polymer fluids

M. Guenza
Department of Chemistry and Institute of Theoretical Science, University of Oregon, Eugene, OR 97403

The Generalized Langevin Equation for the Cooperative Dynamics of interacting polymer chains (M.Guenza, *J.Chem.Phys.* v.110, 7574 (1999)) is implemented to investigate the anomalous dynamics of unentangled polymer melts. The proposed equation of motion formally relates the anomalous center-of-mass diffusion, as observed in computer simulations and experiments, to the nature of the effective intermolecular mean-force potential. An analytical Gaussian-core form of the potential between the centers of mass of two polymers is derived, which agrees with computer simulations and allows the analytical solution of the equation of motion. The calculated center-of-mass dynamics is characterized by an initial subdiffusive regime that persists for the spatial range of the intermolecular mean-force potential, and for time intervals shorter than the first intramolecular relaxation time, in agreement with experiments and computer simulations of unentangled polymer melt dynamics.

I. INTRODUCTION

The dynamics of simple fluids (e.g. monoatomic or colloidal) is driven by the fluid-mediated interactions between the particles as they move under the influence of the "effective" potential of mean-force. The potential of mean-force is related to the "static" radial distribution function $g(r)$, which describes the probability of finding another particle at some distance r from the first "tagged" particle. The structure of the fluid, and the shape of $g(r)$, depends on the strength and shape of the "bare" interparticle potential, so that the nature of the interparticle interactions completely defines the static and dynamical properties of the fluid. [1]

For molecular fluids, the liquid structure and dynamics become more complex as they are driven by the interplay between intermolecular and intramolecular interactions. [1,2] However, for high molecular weight fluids such as polymer melts, the description is again conventionally simplified by assuming that the intramolecular forces dominate the intermolecular forces due to chain connectivity. In this case, the dynamics of a single chain is described by a Generalized Langevin Equation (GLE) where the surrounding fluid acts as a mean-field medium that interacts with the "tagged" molecule only through the effective friction coefficient and the random intermolecular forces. Specifically, unentangled polymer fluids are described by the Rouse equation, an "intramolecular" GLE where the memory function is neglected. [3]

The Rouse equation has proved very successful in explaining several experimental findings of unentangled polymer fluid dynamics. [4] It correctly predicts the scaling with degree of polymerization of the diffusion coefficient and bulk viscosity. Nevertheless, it appears to fail in describing the center-of-mass (c.o.m.) anomalous dynamics experimentally observed for $t \leq \tau_{Rouse}$, with $\tau_{Rouse} = R_g^2/D_{Rouse}$ the first Rouse relaxation time. Here $R_g = l\sqrt{N/6}$ is the molecular radius-of-gyrations, with N the degree of polymerization, and l the statistical segment length. The Rouse diffusion coefficient $D_{Rouse} = k_B T/(N\zeta)$, where k_B is Boltzmann's constant, T is the absolute temperature, and ζ is the Rouse monomer friction coefficient. In the short-time regime ($t \leq \tau_{Rouse}$) the Rouse equation predicts linear-in-time purely diffusive c.o.m. dynamics, while the observed c.o.m. mean-square displacement follows a subdiffusive regime ($\Delta R^2(t) \propto t^\nu$), with $\nu \approx 0.75 - 0.9$, which crosses-over to the free Rouse diffusion ($\Delta R^2(t) \propto t$) at $t \approx \tau_{Rouse}$. [5–7] A subdiffusive regime has been observed also in melts of entangled polymer chains for time shorter than the entanglement time, t_e (for $t \geq t_e$ the polymer motion is restricted to a curvilinear diffusion) where the conditions for Rouse dynamics - purely diffusive behavior - would seem to hold. In polymer solutions, the subdiffusive dynamics only appears above the overlap concentration, c^* [8,9], suggesting that this effect is driven by intermolecular forces. [5,6]

The failure of the Rouse approach in the short-time regime is actually not surprising. The underlying assumption of this model is that the dynamics of the surrounding fluid, and hence the intermolecular time correlation functions, relax on a time scale much shorter than any of the intramolecular processes. This allows the minimization of the memory contribution resulting from the projection of the fluid dynamics onto the intramolecular coordinates, defined as the slow variables in the system. [10] In polymer melts and concentrated polymer solutions, this assumption obviously does not hold, since there is no separation of time scales between intramolecular and intermolecular relaxations. The characteristic time of intermolecular relaxation, τ_{inter}, is defined as the time required for the polymer to escape from the influence of the intermolecular potential of mean-force. In polymer fluids the range of the potential is given by the extension of the "correlation hole" [11] in the pair-distribution function, which is of the order of the molecular radius-of-gyration, R_g. Thus, τ_{inter} appears to be of the same order of magnitude of the longest intramolecular

relaxation time, $\tau_{inter} \approx \tau_{Rouse}$. As a consequence in the time region $t \leq \tau_{Rouse}$, where the intermolecular correlation functions have not yet decayed to zero, we expect the dynamics to be substantially affected by the intermolecular effects, and the Rouse equation should not hold.

The correction due to intermolecular effects becomes more relevant in melts of high molecular weight polymer chains since it depends on the number of interacting polymers to be found on average within the range of the potential, $n \approx \rho l^3 \sqrt{N}$. Intermolecular effects also increase with the number of molecules undergoing cooperative dynamics, when the system approaches its glass transition. [12]

While the theoretical approach to the structure of the macromolecular fluid has been successfully implemented through a rigorous formalism to include at the same level of detail both intramolecular and intermolecular interactions [13], the rigorous, non phenomenologycal, upgrade of the dynamics appears quite challenging. Our approach is in this direction. [14] We derive a GLE from the first-principles Liouville equation by projecting the dynamics [1] on a set of variables given by the coordinates of the molecules undergoing slow cooperative dynamics. [14] Polymer melts are dynamically heterogeneous, and it is possible to observe interconverting regions of slow and fast dynamics. [15] When projecting on the group of slow interacting polymers, the projection approximation, together with the mean-field description of the liquid of fast molecules, becomes well justified. The derived GLE describes the dynamics of a polymer chain inside a dynamically heterogeneous melt. The equation explicitly includes intramolecular and intermolecular forces in both the frequency term and the memory function. The traditional single-polymer GLE is recovered when the fluid is described as a mean-field continuum, i.e. the pair distribution function $g(r) = 1$. In the opposite limit of two interacting structureless particles, the equation recovers the well known GLE, extensively studied in the past. [16] Thus, the equation holds in both the well-known opposite limits of dominant intramolecular or intermolecular interactions.

Starting from the Cooperative Dynamics Generalized Langevin Equation (CDGLE), we investigate here the anomalous c.o.m. dynamics for an unentangled polymer chain inside a dynamically heterogeneous melt. In section II we present an analytical Gaussian core expression for the intermolecular c.o.m. potential between two interacting polymers which allows an analytical solution of the GLE through a normal modes analysis. Anomalous scaling exponents and asymptotic values for the c.o.m. dynamics are presented in Section III, together with numerical model calculations. The comparison of the theory with computer simulation data of unentangled c.o.m. dynamics follows in Section IV. A brief discussion concludes the paper.

II. CENTER-OF-MASS COOPERATIVE DYNAMICS, AND INTERMOLECULAR POTENTIAL

We start from the CDGLE for the dynamics of a single polymer chain in a structurally homogeneous, but dynamically heterogeneous fluid. An effective segment of index a, in a polymer of index i, follows [14]

$$\begin{aligned}\zeta_0 \frac{d\mathbf{r}_a^{(i)}(t)}{dt} = \frac{1}{\beta} \frac{\partial}{\partial \mathbf{r}_a^{(i)}(t)} \ln[\prod_{j=1}^{n} \Psi(\mathbf{r}^{(j)}(t)) \\ \prod_{k<j}^{n} g(\mathbf{r}^{(j)}(t) - \mathbf{r}^{(k)}(t))] - \frac{\beta}{3} \sum_{b\neq a}^{N} \int_0^t d\tau < \mathbf{F}_a^{(i)} \cdot \mathbf{F}_b^{Q(i)}(t-\tau) > \frac{d\mathbf{r}_a^{(i)}(\tau)}{d\tau} \\ -\frac{\beta}{3} \sum_{b=1}^{N} \sum_{j\neq i}^{n} \int_0^t d\tau < \mathbf{F}_a^{(i)} \cdot \mathbf{F}_b^{Q(j)}(t-\tau) > \frac{d\mathbf{r}_a^{(i)}(\tau)}{d\tau} + \mathbf{F}_a^{Q(i)}(t) \ ,\end{aligned} \tag{1}$$

where $\Psi(\mathbf{r}^i(t))$ is the intramolecular distribution function, $-\beta^{-1} ln g[\mathbf{r}^j(t), \mathbf{r}^k(t)]$ is the intermolecular potential of mean-force between two sites (monomers) belonging to two different polymers, and $\beta = (k_B T)^{-1}$. $\mathbf{F}_a^{Q(i)}(t)$ is the projected random force ($Q = 1 - P$, where P is the projection operator [1,14]) that represents the random collision with the surrounding fluid. This Generalized Langevin equation is non linear, and couples the dynamics of the interacting chains through the intermolecular contributions included in the frequency term and in the memory function. The equation cannot be solved analytically, unless a set of approximations is introduced.

For unentangled polymer melts the equation can be simplified, since the corrections due to the memory function contributions can be in first approximation neglected for several reasons. Because our approach derives the Langevin equation by projecting the Liouvillian dynamics over the extended set of basis functions (not only *intram*olecular polymer coordinates as in the derivation of the Rouse equation, but also *inter*molecular coordinates) the memory function corrections are further minimized with respect to the conventional intramolecular single chain description. [1]

The purely intramolecular equation reduces to the Rouse equation when memory function contributions are neglected. [3] The Rouse equation is already a reasonable approximation to the single polymer dynamics, and is correct in the long-time regime. It is commonly accepted that when the memory function contribution is included, the intramolecular diffusive equation describes the cross-over to entangled polymer dynamics. [17,18]

When the memory function contributions are neglected and we focus on the single chain center-of-mass dynamics for an unentangled polymer chain of index i, Eq.(1) reduces to

$$\zeta \frac{d\mathbf{r}^{(i)}_{c.m.}(t)}{dt} = \frac{1}{\beta} \frac{\partial}{\partial \mathbf{r}^{(i)}_{c.m.}(t)} \ln[\prod_{j=1}^{n} \prod_{k<j}^{n} g(\mathbf{r}^{(j)}_{c.m.}(t) - \mathbf{r}^{(k)}_{c.m.}(t))] + \mathbf{F}^{(i)}_{c.m.}(t) \ , \tag{2}$$

since the c.o.m. diffusion is decoupled from the internal relaxation dynamics. $-\beta^{-1} ln g[\mathbf{r}^j(t), \mathbf{r}^k(t)]$ is the intermolecular potential of mean-force between the c.o.m. belonging to two different polymers, ζ is an effective friction coefficient, and $< \mathbf{F}^{(i)}_{c.m.}(t) \cdot \mathbf{F}^{(j)}_{c.m.}(0) >= 6\zeta\beta^{-1}\delta(t)$ the fluctuation-dissipation condition.

A. Effective Gaussian-core potential between two interacting polymers

To pursue on analytical solution of Eq.(2) we derive an analytical, Gaussian-core expression for the intermolecular potential between the c.o.m. of a pair of polymers. The modeling of polymer coils as interpenetrable soft spheres with a realistic Gaussian-core potential has been a subject of long-standing interest. In addition to the obvious scientific relevance [19], such an approach could significantly reduce the computational time required in the simulations of polymer fluids. [20] For polymer solutions, a mean-field derivation of the potential for interpenetrating polymers was obtained by Flory and Krigbaum. [21] Their mean-field approach predicts a potential at contact that increases with N, in disagreement with computer simulations where the contact potential decreases with increasing N. An alternative derivation through scaling theory [22] and renormalization group calculations [23], recovers the correct scaling exponent in the asymptotic $N \to \infty$ regime. In a recent series of papers Hansen and coworkers presented an empirical form of the potential in the finite-size regime [24], and showed, by comparison with computer simulations, that the Gaussian-core model gives a very good description of the interpolymer potential in a wide range of densities and temperatures. The same study also pointed out that interactions of higher order than the effective pair interactions do not give relevant contributions to the calculation of the thermodynamic properties of the fluid in the semidilute regime.

We derive here a Gaussian-core pair potential for the interaction between the c.o.m. of two interacting polymers in a melt. The potential is calculated as a function of the c.o.m. interpolymer distance, $R(t) = |\mathbf{R}(t)|$. If $\mathbf{r}^{(i)}_a$ is the position of monomer a in chain i with respect to its c.o.m. coordinates, and $\mathbf{r}^{(j)}_b$ is the position of monomer b in chain j in the same coordinate system, the distance between a and b is given by $\mathbf{r} = \mathbf{r}^{(j)}_b + \mathbf{R}(t) - \mathbf{r}^{(i)}_a$. At any instant the segments are statistically positioned around the c.o.m. following a Gaussian distribution [25]

$$\Psi(r_a) = \left(\frac{3}{2\pi R_g^2} \right)^{3/2} e^{\frac{-3\mathbf{r}_a^2}{2R_g^2}} \ . \tag{3}$$

The distance between the polymers' c.o.m. is exactly obtained from the integral $\mathbf{R} = \int d\mathbf{r}^{(i)}_a \Psi(r^{(i)}_a) \int d\mathbf{r}^{(j)}_b \Psi(r^{(j)}_b)\mathbf{r}$.

In analogy with the previous calculation, the c.o.m. pair distribution function, $g(R)$, is calculated by averaging over the monomer positions, the four-point distribution function which correlates two monomers on different polymers, and their c.o.m.. The four point distribution function is approximated by the product of three two-point distribution functions according to $g(R) \approx \int d\mathbf{r}^{(i)}_a \Psi(r^{(i)}_a) \int d\mathbf{r}^{(j)}_b \Psi(r^{(j)}_b) g(r)$. For the monomer pair distribution function, we adopt the polymer thread-model form, which has been shown to reproduce many fundamental features of the polymer melt structure [13],

$$g(r) = 1 + \xi_\rho \left[\frac{e^{-r/\xi_\rho}}{r} - \frac{e^{-r/\xi_c}}{r} \right] \ . \tag{4}$$

Two characteristic lengths enter the equation: the local density screening length $\xi_\rho = 3l/(\pi\rho^*)$ with $\rho^* = \rho l^3$ the reduced fluid density, and the correlation hole length scale $\xi_c = R_g/\sqrt{2}$. In the "thread" model the chain is composed of beads of vanishing thickness, while the "bare" interpolymer interactions are simple hard core repulsions accounted

for by the condition that the site-site pair correlation function vanishes at contact [$g(d) = 0$], while the intermolecular direct correlation function $c(r) = c_0\delta(r)$.

We solve the integral introducing the Fourier transform

$$\frac{1}{r} = \frac{4\pi}{(2\pi)^3}\int d\mathbf{k}\frac{e^{i\mathbf{k}\cdot\mathbf{r}(t)}}{k^2} \ , \tag{5}$$

and integrating over the coordinates of the two monomers. The c.o.m. pair distribution function

$$g(R) \approx 1 + \xi_\rho \frac{2}{\pi}\frac{1}{R}\int_0^\infty dk k \sin(kR)\left[\frac{\xi_c^{-2} - \xi_\rho^{-2}}{(\xi_\rho^{-2} + k^2)(\xi_c^{-2} + k^2)}\right] e^{-k^2R_g^2/3} \ . \tag{6}$$

The exponential terms are dominat for $k^2 \leq N^{-1}$, which implies $k^2\xi_\rho^2 \leq N^{-1}$ and $k^2\xi_c^2 \leq 1$. This approximation simplifies the previous equation to

$$g(R) \approx 1 + \xi_\rho\left[\xi_\rho^2 - \xi_c^2\right]\sqrt{\frac{2}{\pi}}\left(\frac{3}{2R_g^2}\right)^{3/2} e^{-\frac{3R^2}{4R_g^2}} \tag{7}$$

By keeping the first order term in the expansion of the logarithm and introducing the definitions of ξ_ρ and ξ_c, the approximate solution for the interpolymer potential between two polymers of large, finite N becomes

$$w(R) = -\log g(R) \approx \frac{27\sqrt{2}}{4\pi\sqrt{\pi}}\frac{1}{\sqrt{N}\rho^*}[1 - 108\pi^{-2}(\rho^*)^{-2}(N)^{-1}]e^{-3R^2/(4R_g^2)} \ . \tag{8}$$

$w(R)$ is Gaussian and finite at all interpolymer distances, with a range of the order of the radius of gyration. At full polymer-polymer overlap, $w(0)$ decreases with increasing reduced fluid density, ρ^*, reflecting the transition from compressible to incompressible systems. It also decreases with increasing polymer molecular weight due to the increasing interpenetrability of the polymer chains. Eq.(8) is in qualitative agreement with the trend observed in computer simulations of semidilute polymer solutions. The last section of the paper shows that Eq.(8) is in good agreement with data from computer trajectories provided by Grest [7] for polymer melts at different temperature, density, and molecular weight.

The derived interpolymer potential belongs to the class of bounded interaction potentials that do not diverge at the origin. [19] Such potentials arise naturally as effective interactions between the c.o.m. of soft, flexible macromolecules since the c.o.m. of two molecules can coincide without violation of the excluded volume conditions. At complete polymer overlap, the $N \to \infty$ scaling limit of $w(0)$ is not finite in disagreement with the observed behavior in semidilute solutions. However a comparison with computer simulations for the melt is not possible in this study since our data do not reach the $N \to \infty$ scaling regime.

B. Many-chain center-of-mass dynamics

To include the pair intermolecular potential just derived in Eq.(1), several steps need to be undertaken. Since it is the distinct part of the Van Hove function that appears in Eq.(**??**, we assume a time-dependence of the potential, which enters through the evolution of the square intermolecular distance between the c.o.m. of the two polymers, $R^2(t)$. The intermolecular term in Eq.(1) results from the decomposition of the n N body distribution function in the product of intra- and inter-molecular pair distribution functions. [14] In principle this high order distribution function is not equivalent to the product of two-body terms. However a decomposition in pair potentials is the natural approximation to adopt, and in our case it is supported by the quantitative agreement with the simulation data. The product of the pair distribution functions gives n equivalent terms in Eq.(2). The intermolecular force for a group of $n \approx \rho^*\sqrt{N}$ interacting polymer chains is

$$G(t)R(t) \approx \frac{81\sqrt{2}}{8\pi\sqrt{\pi}}R_g^{-2}[1 - 108\pi^{-2}(\rho^*)^{-2}(N)^{-1}]e^{-3<R^2(t)>/(4R_g^2)}R(t) \ . \tag{9}$$

The intermolecular distance is approximated by its statistical average over the polymer configurational space, $< R^2(t) >$, and in the many-chain description becomes $< R^2(t) > \approx n\Delta R^2(t) - 6D_\chi t$, where $\Delta R^2(t)$ is the single chain mean-square displacement. $D_\chi = D_{Rouse}/(\rho^*\sqrt{N})$ is the collective diffusion coefficient derived below. The

approximate effective potential that corresponds to the force in Eq.(9), is found to be in good agreement with the time-dependent potential from computer simulations, as discussed in the last section of the paper.

Eq.(2), with Eq.(9), reduces to a set of coupled equations of motion for the c.o.m. polymer dynamics

$$\zeta \frac{d\mathbf{r}_{c.m.}^{(i)}(t)}{dt} = G(t)[\mathbf{r}_{c.m.}^{(i)}(t) - R^{cm}(t)] + \mathbf{F}_a^{Q(i)}(t) \ , \tag{10}$$

where $R^{cm}(t) = n^{-1}\sum_{j=1}^{n} \mathbf{r}_{cm}^{(j)}(t)$ is the coordinate of the c.o.m. position for the dynamical heterogeneity. Eq.(10) has the advantage of including both the intramolecular and the intermolecular forces while keeping the mathematical simplicity of the Rouse equation, and it can be solved analytically by transformation into normal modes of motion.

Because of the symmetry of the system, composed by equivalent polymer chains, the set of coupled equations of motion reduces to two independent equations in the relative, $\mathbf{r}_\xi(t) = 2^{-1/2}[\mathbf{r}_{cm}^{(i)}(t) - \mathbf{r}_{cm}^{(j)}(t)]$, and collective coordinates, $\mathbf{r}_\chi(t) = n^{-1/2}\sum_{i=1}^{n} \mathbf{r}_{cm}^{(i)}(t)$.

$$\zeta \frac{d\mathbf{r}_\xi(t)}{dt} = G(t)\mathbf{r}_\xi(t) + \mathbf{F}^\xi(t) \ , \tag{11}$$

$$\zeta \frac{d\mathbf{r}_\chi(t)}{dt} = \mathbf{F}^\chi(t) \ . \tag{12}$$

The relative and collective projected force correlation functions in the Markov limit obey the fluctuation-dissipation conditions

$$< \mathbf{F}_\alpha^\xi(t) \cdot \mathbf{F}_\gamma^\xi(t') >= 6\zeta\beta^{-1}\delta(t-t')\delta_{\alpha\gamma} \ , \quad < \mathbf{F}_\alpha^\chi(t)\mathbf{F}_\gamma^\chi(t') >= 6\zeta\beta^{-1}\delta(t-t')\delta_{\alpha\gamma} \ . \tag{13}$$

Eqs.(11, 12) are exactly solved through standard procedures [26,27], and the single chain c.o.m. coordinate, in the ensemble of molecules undergoing correlated dynamics, is obtained from the combination of the collective and relative contributions.

III. CENTER-OF-MASS DYNAMICS: ASYMPTOTIC BEHAVIOR AND MODEL CALCULATIONS

The single-chain mean-square displacement of the c.o.m. becomes

$$\begin{aligned} \Delta R^2(t) &= < \left(\mathbf{R}_{c.m.}(t) - \mathbf{R}_{c.m.}(0)\right)^2 >= \frac{n-1}{n} < \left(\mathbf{r}_\xi(t) - \mathbf{r}_\xi(0)\right)^2 > + \frac{1}{n} < \left(\mathbf{r}_\chi(t) - \mathbf{r}_\chi(0)\right)^2 > \ , \\ &\approx < \left(\mathbf{r}_\xi(t) - \mathbf{r}_\xi(0)\right)^2 > + 6D_{Rouse}t/(\rho\sqrt{N}) \ . \end{aligned} \tag{14}$$

While the collective contribution is linear in time with a constant diffusion coefficient D_χ, the relative contribution exhibits a more complex behavior that depends on the strength of the intermolecular interaction, $G(t)$. From Eq.(9) $G(0)$ is defined as the force at complete polymer overlap.

$$< \left(\mathbf{r}_\xi(t) - \mathbf{r}_\xi(0)\right)^2 > \ = < \mathbf{r}_\xi^2(0) > \left(e^{-\alpha(t)} - 1\right)^2 + 6D_{Rouse}e^{-2\alpha(t)} \int_0^t e^{2\alpha(t')}dt' \ ,$$

where

$$\alpha(t) = \frac{G(0)}{\zeta} \int_0^t e^{-\frac{3<R^2(t')>}{4R_g^2}} dt' = \zeta^{-1} \int_0^t G(t')dt' \ . \tag{15}$$

Interpolymer interactions vanish at long time, $t \gg \tau_d$, where we define τ_d as the characteristic time in which $G(t) \to 0$. In general τ_d describes the time that a molecule has to travel to escape from the range of the intermolecular potential. In uncharged polymer fluids at temperature well above their glass transition, the range of the potential is comparable to R_g, and $\tau_d \approx \tau_{Rouse}$. For $t \gg \tau_d$, the single-chain c.o.m. mean-square displacement recovers Rouse diffusion. For $t \ll \tau_d$, $G(t)$ is a function of intermolecular distance $< R^2(t) >$ and Eq.(14) has to be solved numerically through a self-consistent procedure.

In a few well-defined conditions Eq.(14) is analytically soluble. At short time the single-chain c.o.m. mean-square displacement follows $\Delta R^2(t) \approx 6t/(\beta N\zeta_0) + G(0)^2 < R^2(0) > t^2/(\zeta_0^2)$. If $G(0) \to 0$ it recovers the conventional Langevin dynamics, while, if $|G(0)| > 0$, it recovers a short-time superdiffusive behavior characteristic of Langevin

equations with a time dependent drift coefficient. [26,27] Since Langevin equations only describe overdamped chain dynamics, they do not hold in the short-time region where the dynamics is precollisional. [28] In the present study, we focus on the subdiffusive and free-diffusive c.o.m. dynamics in the postcollisional regime.

The onset of the anomalous subdiffusive regime takes place at the characteristic time $\tau_1 = \frac{\zeta}{2G(0)}$. This suggests that a system with intermolecular interaction of increasing strength "freezes" its dynamics at shorter and shorter times. Equivalently we can say that the motion begins to be suppressed on the largest length scale (smallest index modes of motion), and by increasing $G(0)$ the dynamics is progressively frozen at shorter and shorter length scales, or higher and higher index modes. [29] The increase of the monomer relative friction coefficient has an opposite effect, since it slows down the dynamics and enforces the overdamped regime.

For $t \gg \tau_1$ the dynamics are different depending on the nature of the long-range potential. Since the c.o.m. interpolymer potential results from the combination of monomer-monomer interactions, and in polymer melts excluded volume interactions are dominant, this potential is repulsive. An effective intermolecular long-range attractive component can appear, however, when the single-polymer is constrained, for example because of the presence of chain-chain uncrossability or entanglements. In those cases, the molecule has to overcome an effective potential barrier in order to diffuse. Attractive effective potential are also presents in polymer blends, self-assembling polymer systems, and in droplets of polymer liquids.

If we approximate the infinitesimal mean-square-displacement as linear in time, the interpolymer distance $< \Delta R^2(t) > \approx 6Dt$. When introduced in Eq.(15) it yields

$$\alpha(t) = \frac{2G(0)R_g^2}{9\zeta D}\left(1 - e^{-\frac{9Dt}{2R_g^2}}\right) . \tag{16}$$

For short, highly mobile polymer melts, $9Dt \gg 2R_g^2$, the dynamics is simply diffusive at any time-scale.

In a melt of slowly moving, long polymer chains, $9Dt \ll 2R_g^2$. If the potential is repulsive, the single-chain dynamics crosses over from the subdiffusive regime, which describes the slowing down of the single-chain dynamics due to the presence of the surrounding molecules ("cage effect"), to free single-chain diffusion at $t \approx 2R_g^2/(9D)$, where $\alpha(t)$ becomes constant, $\alpha(t) \approx -2G(0)R_g^2/(9D\zeta)$. A decrease in the polymer molecular weight, or an increase in the chain mobility decreases the duration of the subdiffusive regime.

The c.o.m. dynamics of slowly moving, long polymer chains interacting through an attractive long-range potential, follows a subdiffusive regime at intermediate time. In strongly interacting systems the relative mean-square displacement is constant, $< (\mathbf{r}_\xi(t) - \mathbf{r}_\xi(0))^2 > = < \mathbf{r}_\xi^2(0) > + 3/[N\beta G(0)]$, and the single-chain dynamics is driven by the collective contribution. The surrounding molecules act as a cage of the tagged molecule dynamics. At longer times, when $t \approx 2R_g^2/(9D)$, the single-chain exhibits free Fickian dynamics. This regime corresponds to the molecule's excape from the surrounding "cage", as it overcomes an effective energetic potential barrier. If the time scale of observation is shorter than this dissociation time, the c.o.m. interdiffusion is frozen, and the system behaves non-ergodically.

The asymptotic behaviors just discussed are illustrated by numerical calculations in Figures 1 and 2. We investigate the influence of the intermolecular force, $G(t)$, in the scenarios of attractive and repulsive long-range interactions for long, slowly-moving polymer fluids, $9Dt \gg 2R_g^2$. In short highly mobile polymer chains the anomalous dynamics is less relevant.

Eq.(10), when the definition of $G(t)$ in Eq.(9) is introduced, becomes non linear as the intermolecular potential depends on the interpolymer distance, $R^2(t)$, that changes while the system evolves in time. Thus the short-time dynamics depends on the choice of the initial interpolymer distance. Different values of the distance, however, mainly affect the dynamics in the precollisional regime that is outside the range of validity of our equation. An estimate of the initial interpolymer distance, which is a function of the bulk properties of the fluid, can be obtained from the distribution in space of the polymer chains inside the volume spanned by the potential. The average number of chains in a sphere of radius r, as a function of time, is given by the time-dependent pair distribution

$$n[r(t)] = N^{-1}\int_0^r d\mathbf{r}'\rho g[r'(t)] , \tag{17}$$

which gives for the initial mean-square intermolecular distance inside the range of the potential

$$< R^2(0) > \propto \int_0^{\sim R_g} n[r(0)]r^2 dr \approx R_g^2 . \tag{18}$$

Since the intramolecular monomer distribution is Gaussian the chains inside the potential range are not uniformly distributed, and the resulting average intermolecular distance is of the order of the polymer radius-of-gyration.

To perform quantitative model calculations we specify the numerical value of a few more parameters. The model polymer chain comprises $N = 100$ statistical segments of unitary length l, with the chain described by a freely jointed model consistently with Rouse theory. The effective temperature is set to $k_BT = 1$ in units of $G(0)$, and we assume the density of the melt state, $\rho = 1$. The number of chains initially correlated inside the range of the potential is given by Eq.(17) as $n \approx 4/3\pi\sqrt{N}l^3\rho$. n is also the number of chains undergoing correlated motion, defined from Eq.(1) as the number of chains interacting through the mean-force potential. The effective time-independent monomer friction coefficient is set to $\zeta = 1$.

In Figures 1 and 2, we study the decay in time of the interaction strength, $G(t)$, when its value at complete polymer overlap, $G(0)$, is varied for a system of slowly moving, high molecular weight polymers. We use as an effective parameter the interaction strength, $G'(0)$, that is a multiple of $G(0)$ calculated from Eq.(9). The features emerging from those plots are related to the onset of anomalous dynamics in the c.o.m. mean-square displacement as a function of time. In general an increase of the strength of the potential induces the onset of anomalous dynamics.

$G(t)$ is normalized by its own value calculated when $< R^2(t) >= R_g^2$, i.e. $G(t)|_{R_g}$. For small $|G(0)|$, the decay of $G(t)$ follows a single step mechanism that corresponds to a mean-square displacement approaching the linear single-chain diffusion. For large $|G(0)|$ the behavior depends on the sign of the potential.

For a repulsive intermolecular potential (Figure 1) an increase of $G(0)$, for $t \leq \tau_{Rouse}$, induces the onset of a stretched exponential decay which crosses over to Rouse behavior at $t \approx \tau_{Rouse}$. In the c.o.m. mean-square displacement, the presence of the interactions modifies the Rouse free diffusive behavior by inducing a subdiffusive behavior at short time. At $t \gg rR_g^2/(9D)$ the system recovers free Fickian diffusion. No many-chain correlated dynamics appears at long time.

To investigate the effect of an attractive effective potential we adopt $G'(0)$ equal to a multiple of $G(0)$, defined by Eq.(9), assuming a minus sign. At intermediate time the system is frozen in a metastable equilibrium configuration with constant strength of the interactions, and constant interpolymer distance (see Figure 2). This regime corresponds to an anomalous subdiffusive regime ($\Delta R^2(t) \propto t^\nu$ with $\nu \ll 1$). If the thermal energy of the system is high enough, $\beta G'(0) \to 0$, the molecule can escape from the "caged" dynamics reestablishing the effective ergodicity of the system. Otherwise, the system undergoes many-chain correlated dynamics, so it behaves non-ergodically. Thus, by increasing the strength of the intermolecular potential the theory predicts an apparent ergodic to non-ergodic transition.

In the Figures are also illustrated the two limiting cases of a single-chain free dynamics ($G(0) = 0$), and for the "caged" collective dynamics ($G(0) \to \infty$). The comparison with those curves emphasizes how the single-chain dynamics in strongly interacting attractive systems crosses over from the short-time single-chain dynamics to the collective many-chain diffusion at long time.

IV. COMPARISON WITH SIMULATIONS

To test our approach we compare its predictions with computer simulations of unentangled polyethylene (PE) dynamics in the melt state and at decreasing temperature, while approaching the glass transition (the entanglement degree of polymerization $N_e = 136$). PE has been extensively investigated experimentally [29,30] because of its industrial applications, and has been chosen as a model system for computer simulations [5–7] due to the simplicity of its monomer structure. We first compare with data from computer simulations performed by Grest and coworkers. [7] The simulations calculate the dynamics at constant volume and constant temperature, using the experimental densities at atmospheric pressure, as reported in Table I.

We use as an input to the theory the density, polymer molecular weight, number and length of the statistical segments from computer simulations (see Table I). Figure 3 shows very good agreement between theory and simulations, when one fitting parameter, i.e. the potential at complete interpolymer overlap $w'(0)$, is optimized. Table I reports the ratio between the optimized analytical values of $w'(0)$ and the theoretical values, $w(0)$, calculated from Eq.(8). $w'(0)$ appear to be fairly close to $w(0)$. The agreement with the computer simulations is good for all the samples considered, which span a wide range of temperatures and molecular weights.

A second approximation, implicitly introduced in the solution of the CDGLE, is the averaging of the instantaneous interpolymer distance in the effective potential, and the self-consistent solution of Eq.(10). In Figures 4a, 4b, and 4c we present a comparison between Eq.(8) and the time-dependent intermolecular potential between the c.o.m. of two polymers, extracted from computer simulations as $-\ln g[R(t)]$ for the $C_{30}H_{62}$ sample. The approximate static interpolymer potential appears to reproduce quite well the data at any time scale. This is because the time dependence of the potential is quite weak initially, so that the data during the first 30 ps almost superimpose, and are well reproduced by the same analytical formula. In Figure 4d we compare Eq.(8) with the averaged time-dependent Gaussian potential, corresponding to Eq.(9), calculated self-consistently with Eq.(10). The two potentials show

very good agreement. For time intervals larger than 30 ps, when the potential starts to differ significatively at short-distance, the molecules have already diffused to large intermolecular distance and the approximated analytical form of the potential still reproduces well the data.

From the analytical solution of Eq.(10) we calculate the c.o.m. mean-square displacement. The overlap value of the intermolecular potential, $w'(0)$, is fixed from the previous analysis. From the long time diffusion coefficient we derive the value of the effective friction coefficient, reported in Table I. Figure 5 shows that the comparison between simulations and analytical theory gives an excellent agreement in the whole range of space and time scales investigated. This suggests that both the self-consistent procedure and the approximation of neglecting the memory functions contribution are reasonable first-order approximations for unentangled melt dynamics.

A. Unentangled undercooled polymer melt center-of-mass dynamics

We now compare our approach with data from computer simulations of undercooled polymer systems. In a recent paper Binder and coworkers [31] investigated by computer simulations the onset of short-time anomalous dynamics for a melt of unentangled polymer chains. They performed Dynamical Monte Carlo computer simulations at decreasing system temperature, using the bond fluctuation model [32] of a chain of $N = 10$ statistical segments. For this model, which is found to reproduce correctly the dynamics of polymer melts, Binder reports the unit of the single time step (1 Monte Carlo Step $\approx 10^{-13}$ s) and the space unit (1 lattice unit ≈ 2.3 $\mathring{A}$). [33] The chain of $N = 10$ effective segments simulated here, corresponds to a polyethylene chain of $N \approx 50$ bonds of length $l = 1.54$ $\mathring{A}$. [34] Since the model used to simulate the "freezing" of the dynamics privileges stretched bond configuration, the polymer radius-of-gyration slightly increases with decreasing temperature. [35]

We fit the c.o.m. mean-square displacement having as an input to the equation the simulation parameters. The monomer friction coefficient is obtained from the diffusion coefficient in the long-time Rouse regime and is kept constant in all the calculations. We do not include the memory function corrections [36] which in our calculations are negligible for $N \leq N_e$. Because of the approximations involved in the calculations, we don't strongly rely on the precision of the numerical values obtained from the fitting procedure, however the theory makes some interesting suggestions on the physics involved in the process.

In Figure 6 we show that the fitting procedure gives a reasonable agreement between the theory and the data in the complete range of time (length) scale investigated. At high temperature ($k_BT = 1, 0.4$) the dynamics is driven by repulsive interactions in agreement with our previous calculations. The repulsive potential induces a subdiffusive regime that crosses over to the single chain free diffusion. In the simulation the decrease of the diffusion coefficient, follows the empirical Vogel-Fulcher law [31], while the Rouse equation holds for the monomer local dynamics. To obtain a good quantitative agreement with the simulations we use two fitting parameters: the strength of the potential at complete polymer superposition, $w(0)$, and the number of polymer chains undergoing cooperative dynamics, n. The best fit with the data is found for $n = 13$ and $n = 15$, respectively at $k_BT = 1$ and $k_BT = .4$. These values are very close to the theoretically predicted value. For temperatures close to the melt state the system behaves consistently with the study presented above.

When the temperature of the system is further decreased ($k_BT = 0.23, 0.19$) the subdiffusive behavior appears to have a different physical origin than in the high temperature limit. The simulations show an "extremely slow motion", visible also in the monomer mean-square displacement, which is defined to be a "cage effect". [31] From our calculations this regime emerges as a diffusive process involving the correlated dynamics of many-chains. In this regime the polymer chain is caged by the presence of the other polymers and cooperative many-chain dynamics takes place, which indicates an attractive effective potential. While the monomer friction coefficient is constant from the high temperature regime, the number of polymer chains undergoing correlated dynamics increases with decreasing system temperature, in agreement with experimental studies. [15,37,38] This effect would indicate an increase of the range of the dynamical correlation that would correspond to longer range oscillations in the "real" mean-force potential and in $g(r)$. From the fit to the long-time collective diffusion coefficient we obtain $n \approx 25$ for $k_BT = .23$ and $n \approx 300$ for $k_BT = .19$. These results suggest that the freezing of the dynamics is related to a rapid increase in the number of polymer chains involved in the correlated dynamics. In this region of temperature the polymer has to escape from the influence of the intermolecular potential, overcoming an effective potential barrier, through a process which is highly cooperative, and this becomes increasingly difficult at lower temperature.

V. CONCLUSIONS

The presence of effective intermolecular interactions significantly modifies the single-chain dynamics in the short time, local space regime, $\tau_0 \ll t \ll \tau_{Rouse}$. The onset of anomalous dynamics, observed in computer simulations of polymer fluids in the short-time region where the Rouse equation breaks down, appears to be quantitatively related to the presence of the effective mean-force potential. The spatial extent of the anomalous dynamics corresponds to the range of the mean-force potential ($\approx R_g$ in polymer melts well above T_g), while the time scale that characterizes the anomalous dynamics is given by the time necessary for a polymer to escape from the influence of the intermolecular potential ($t \approx \tau_{Rouse}$).

The subdiffusive dynamics at time scale $\tau_1 \ll t \ll \tau_{Rouse}$, corresponds to a slowing down or arrest of the dynamics due to the presence of intermolecular forces. It appears to be a cross-over regime to the long-time diffusive dynamics, consistent with computer simulations where a wide range of exponents is measured . [5–9]

The sign of the intermolecular potential qualitatively modifies the long-range anomalous dynamics. The theory quantitatively reproduces the experimental data in the complete range of time and spatial scales investigated.

VI. ACKNOWLEDGMENTS

We are grateful to G.S.Grest for sharing the trajectories of his computer simulations. Acknowledgment is made to the donors of The Petroleum Research Fund, administrated by the ACS, for partial support of this research. We also acknowledge the support of the National Science Foundation under the grant DMR-9971687.

---

[1] Hansen,J.P.; McDonald, I.R. *Theory of Simple Liquids* Academic Press: London, 1991.
[2] Chandler, D.; Andersen, H.C. *J.Chem.Phys* **1972**, *57*, 1930.
[3] Bixon, M.; Zwanzig, R. *J.Chem.Phys.* **1978**, *68*, 1896.
[4] Doi, M.; Edwards, S.F. *The Theory of Polymer Dynamics* Oxford University Press: Oxford, 1986.
[5] Paul, W.; Yoon, D.Y.; Smith, G.D. *J.Chem.Phys.* **1995**, *103*, 1702; Paul, W.; Smith, G.D.; Yoon, D.Y.; Frago, B.; Rathgeber, S.; Zirkel, A.; Willner, L.; Richter, D. *Phys.Rev.Lett* **1998**, *80*, 2346.
[6] Kopf, A.; Dunweg, B.; Paul, W. *J.Chem.Phys.* **1997**, *107*, 6945.
[7] M.Mondello, G.S.Grest, J. Chem. Phys. **106**, 9327 (1997). K.S.Kostov, K.F.Freed, E.B.Webb III, M.Mondello, G.S.Grest, J.Chem.Phys. **108**, 9155 (1998).
[8] Kremer, K.; Grest, G.S. *J.Chem.Phys.* **1990**, *92*, 5057; Paul, W.; Binder, K.; Heermann, D.W.; Kremer, K. *J.Chem.Phys.* **1991**, *95*, 7726.
[9] Kolinski, A.; Skolnick, J.; Yaris, R. *J.Chem.Phys.* **1987**, *86*, 1567; Smith, S.W.; Hall, C.K.; Freeman, B.D. *Phys.Rev.Lett.* **1995**, *75*, 1316; Smith, S.W.; Hall, C.K.; Freeman, B.D. *J.Chem.Phys.* **1996**, *104*, 5616.
[10] Hansen, J.-P.; McDonald, I.R. *Theory of Simple Liquids* Academic Press: San Diego, 1991.
[11] deGennes, P.G. *Scaling Concepts in Polymer Physics* Cornell University Press: Ithaca, 1979.
[12] Ediger, M.D.; Angell, C.A.; Nagel, S.R. *J.Phys.Chem.* **1996**, *100*, 13200.
[13] Schweizer, K.S.; Curro, J.G. *Adv.Polym.Sci.* **1994**, *116*, 319; Schweizer, K.S.; Curro, J.G. *Adv.Chem.Phys.* **1997**, *97*, 1.a
[14] Guenza, M. *J.Chem.Phys.* **1999**, *110*, 7574.
[15] Ediger, M.D.; Skinner, J.L. *Science* **2001**, *292*, 233, and references therein.
[16] Posch, H.A.; Balucani, U.; Vallauri, R. *Physica* **1984**, *123 A*, 516.
[17] Schweizer, K.S. *J.Chem.Phys.* **1989**, *91*, 5802; *ibid.* **1989**, *91*, 5822.
[18] Hess, W. *Macromolecules* **1987**, *20*, 2587; *ibid.* **1988**, *21*, 2620.
[19] Stillinger, F.H.; Weber, T.A. *Physical Review B* **1980**, *22*, 3790; and references therein.
[20] Dautenhahn, J.; Hall, C.K. *Macromol.* **1994**, *27*, 5399; Murat, M.; Kremer, K. *J.Chem.Phys.* **1998**, *108*, 4340.
[21] Flory, P.J.; Krigbaum, W.R. *J. Chem. Phys* **1950**, *18*, 1086.
[22] Grosberg, A.Y.; Khalatur, P.G.; Khokhlov, A.R. *Makromol. Chem.* **1982**, *3*, 709.
[23] Krüger, B.; Schäfer, L.; Baumgärtner, A. *J.Phys. (Paris)* **1989**, *50*, 319.
[24] Bolhuis, P.G.; Louis, A.A.; Hansen, J.P. *J. Chem. Phys.* **2001**, *114*, 4296; Louis, A.A.; Bolhuis, P.G.; Hansen, J.P.; Maijer, E.J. *Phys.Rev.Lett.* **2000**, *85*, 2522.
[25] Flory P.J. *Statistical Mechanics of Chain Molecules* Hanser Publishers: New York, 1989.
[26] Lillo, F.; Mantegna, R.N. *Physical Review E* **2000**, *61*, R4675.

[27] Risken, H. *The Fokker-Planck Equation* Springer-Verlag: Berlin, 1989.
[28] Balucani, U.; Zoppi, M. *Dynamics of the Liquid State* Oxford Science Publications: Oxford, 1994.
[29] Richter, D.; Willner, L.; Zirkel, A.; Frago, B.; Fetters, L.J.; Huang, J.S. *Phys.Rev.Lett.* **1993**, *71*, 4158.
[30] Pearson, D.S.; Ver Strate, G.; von Meerwall, E.; Schilling, F.C. *Macromolecules* **1987**, *20*, 1133; Pearson, D.S.; Fetters, L.J.; Greassley, W.W.; Ver Strate, G.; von Meerwall, E. *Macromolecules* **1994**, *27*, 711.
[31] Okun, K.; Wolfgardt, M.; Baschnagel, J.; Binder, K. *Macromolecules* **1997**, *30*, 3075; Bennemann, C.; Paul, W.; Binder, K.; Dunweg, B. *Phys.Rev.E* **1998**, *57*, 843.
[32] Binder, K. *Monte Carlo and Molecular Dynamics Simulations in Polymer Science* Oxford University Press: Oxford, 1995.
[33] Binder, K.; Baschnagel, J.; Bennemann, C.; Paul, W. *J.Phys.Cond.Matt.*, **1999**, *11*, A47; Binder, K. in ref.([32]).
[34] Notice that the bond length in the original figure [31] is an effective segment about five times larger than our l.
[35] Paul, W.; Baschnagel, J. in ref.([32]).
[36] A quantitative study of the anomalous dynamics in undercooled polymer fluids needs to include the explicit calculation of the memory function contributions.
[37] Vidal Russell, E.; Israeloff, N.E. *Nature* **2000**, *408*, 695.
[38] Tracht, U.; Wilhelm, M.; Heuer, A.; Feng, H.; Schmidt-Rohr, K.; Spiess, H.W. *Phys. Rev. Lett.* **1998**, *81*, 2727.

TABLE CAPTION

Table I: Simulation and fitting parameters.

$Polymer$	T $[K]$	ρ $[g/cm^3]$	$l[\mathring{A}]$	$w(0)/w'(0)$	$Initial slope$	ζ $[10^9$ dyn $s/cm]$
$C_{10}H_{22}$	298	0.7250	3.26	2	0.97	0.25
$C_{16}H_{34}$	298	0.7703	3.84	.4	0.94	0.44
$C_{16}H_{34}$	323	0.7531	3.75	.6	0.96	0.30
$C_{16}H_{34}$	373	0.7187	3.66	.8	0.97	0.18
$C_{30}H_{62}$	400	0.7421	4.02	.3	0.90	0.21
$C_{44}H_{90}$	400	0.7570	4.18	.3	0.85	0.27

FIGURE CAPTIONS.

Figure 1: a) Normalized intermolecular constant versus normalized time, for various strengths of the repulsive interaction, $G'(0)$. $G'(0)$ is the effective strength at complete polymer overlap from Eq.(9). From the top curve (close to the single-chain diffusion) to the bottom curve: $G'(0) = 0.05\ G(0)$, $0.1\ G(0)$, $0.2\ G(0)$, $G(0)$. $G(0)$ is the intermolecular interaction at initial conditions: $k_BT = 1$ in units of $G(0)$, $N = 100$, $n = \frac{4}{3}\pi\sqrt{N}l^3\rho$, $\rho = 3\ l^{-3}$, and $R^2(0) \approx R_g^2$. Also shown is $G(t)$ for the chain undergoing single chain diffusion. b) Normalized single chain center-of-mass mean-square displacement vs normalized time, at various strengths of $G'(0)$, same values that in Figure 1 a).

Figure 2: a) Normalized intermolecular constant versus normalized time, at decreasing strength of the attractive interaction, $G'(0)$. From the top curve (close to the single-chain diffusion) to the bottom curve: $G'(0) = -0.05\ G(0)$, $-0.067\ G(0)$, $-0.08\ G(0)$, $-0.09\ G(0)$, $-0.1\ G(0)$, $-0.2\ G(0)$, $-G(0)$. Same initial conditions than in Figure 1. Also shown is $G(t)$ for the chain undergoing collective dynamics, and for the single chain diffusion. b) Normalized single chain center-of-mass mean-square displacement vs normalized time, at decreasing $|G'(0)|$, same values than in Figure 2 a).

Figure 3: Comparison between the analytical expression of the soft-core center-of-mass Gaussian potential, Eq.(8), and computer simulations data, vs. the c.o.m. interpolymer distance normalized by the polymer end-to-end distance, R_{ete}, from computer simulations.

Figure 4: Comparison between the analytical equation of the soft-core center-of-mass Gaussian potential, Eq.(8), and the distinct part of the Van Hove distribution function, $-\ln g[R(t)]$, from computer simulations of $C_{30}H_{62}$. Plot vs. the c.o.m. interpolymer distance normalized by the polymer end-to-end distance, R_{ete}, from computer simulations. Curves at a) 10 ps, b) 20 ps, and c) 30 ps. d) Comparison between Eq.(8) and the time-dependent Gaussian potential used in Eq.(10), calculated self-consistently, for 10 ps (square), 20 ps (triangle up), 30 ps (triangle down).

FIG. 5: Center-of-mass mean-square displacement as a function of time. Best fit of the molecular dynamics simulation data (filled circle) with the Rouse equation (dashed line), and with the intermolecular diffusion equation, Eq.(10), for unentangled polymer melts (full line). The short-dashed lines indicate the longest Rouse relaxation time, τ_{Rouse}.

Figure 6: Center-of-mass mean-square displacement as a function of time at $k_BT = 1$ (diamond), $k_BT = 0.4$ (triangle), $k_BT = 0.23$ (square), $k_BT = 0.19$ (circle). Best fit of the simulation data (ref. [31]) with the Rouse equation including intermolecular interactions.

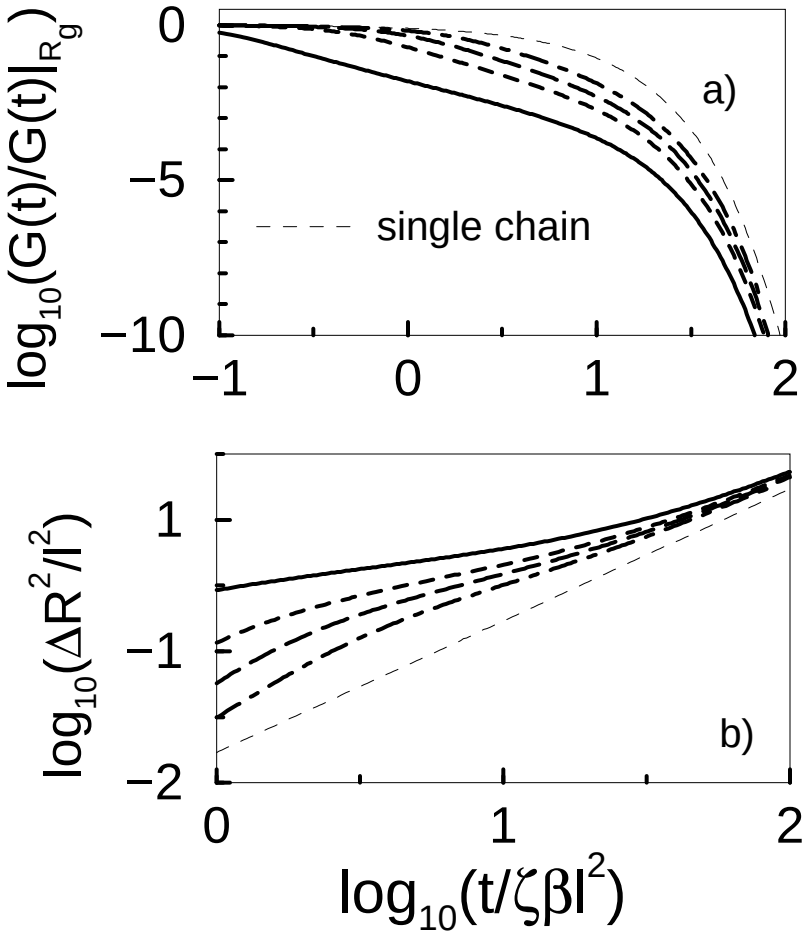

Figure 1 Guenza

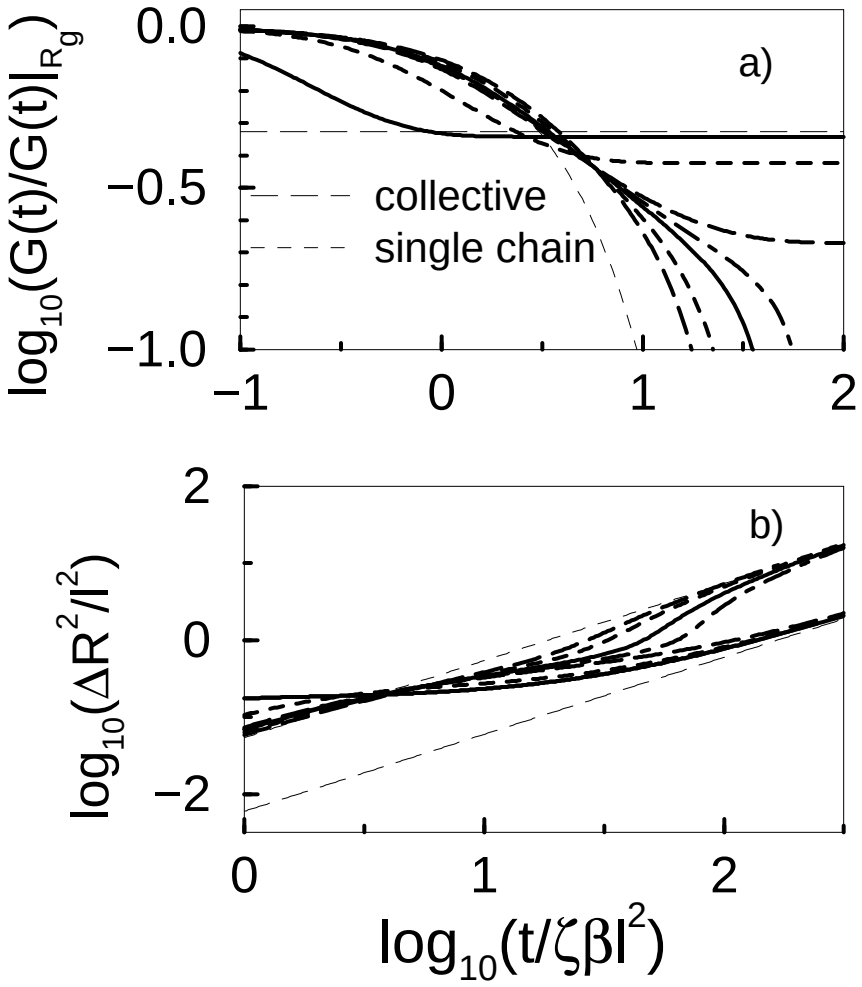

Figure 2 Guenza

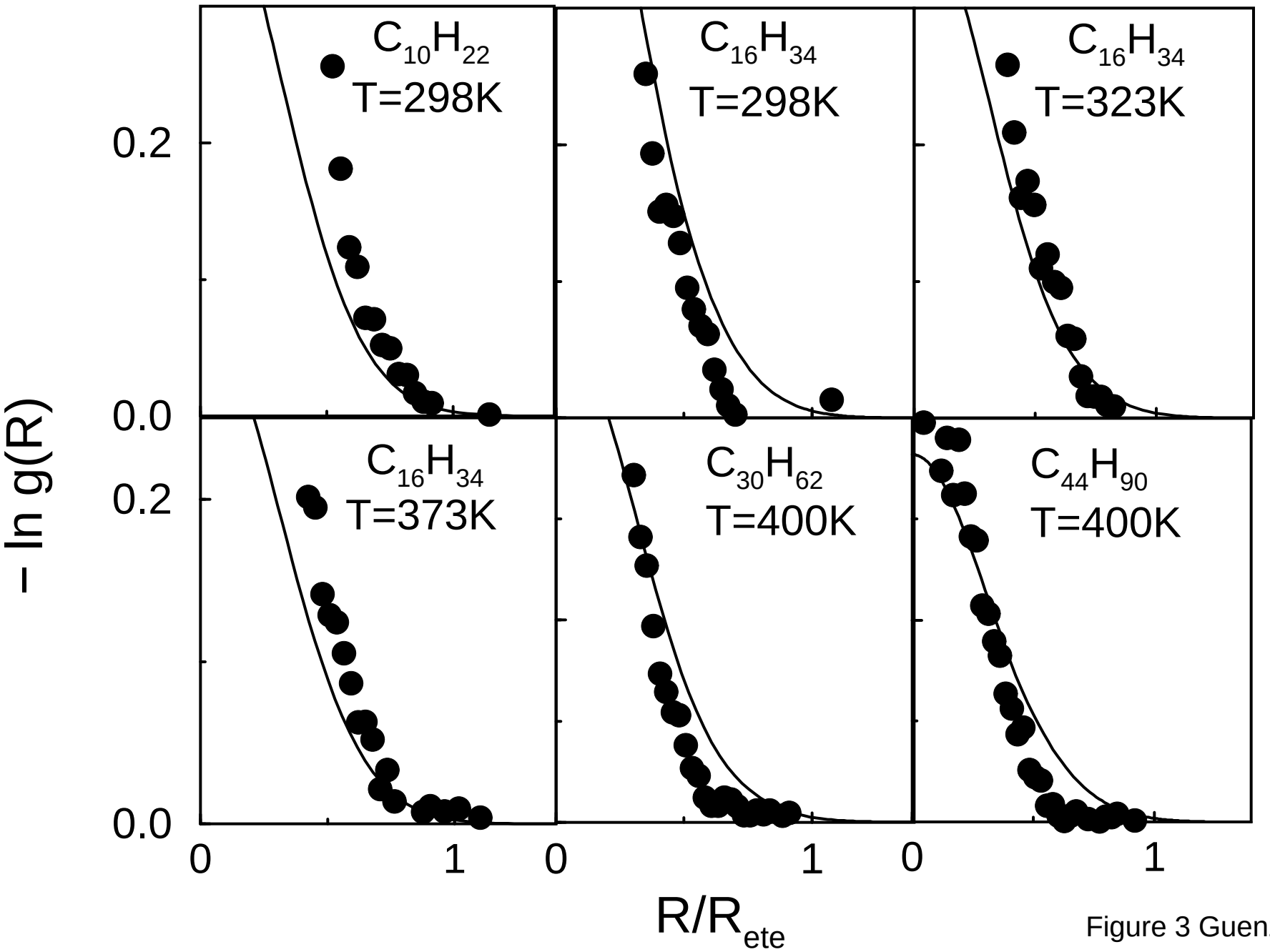

Figure 3 Guenza

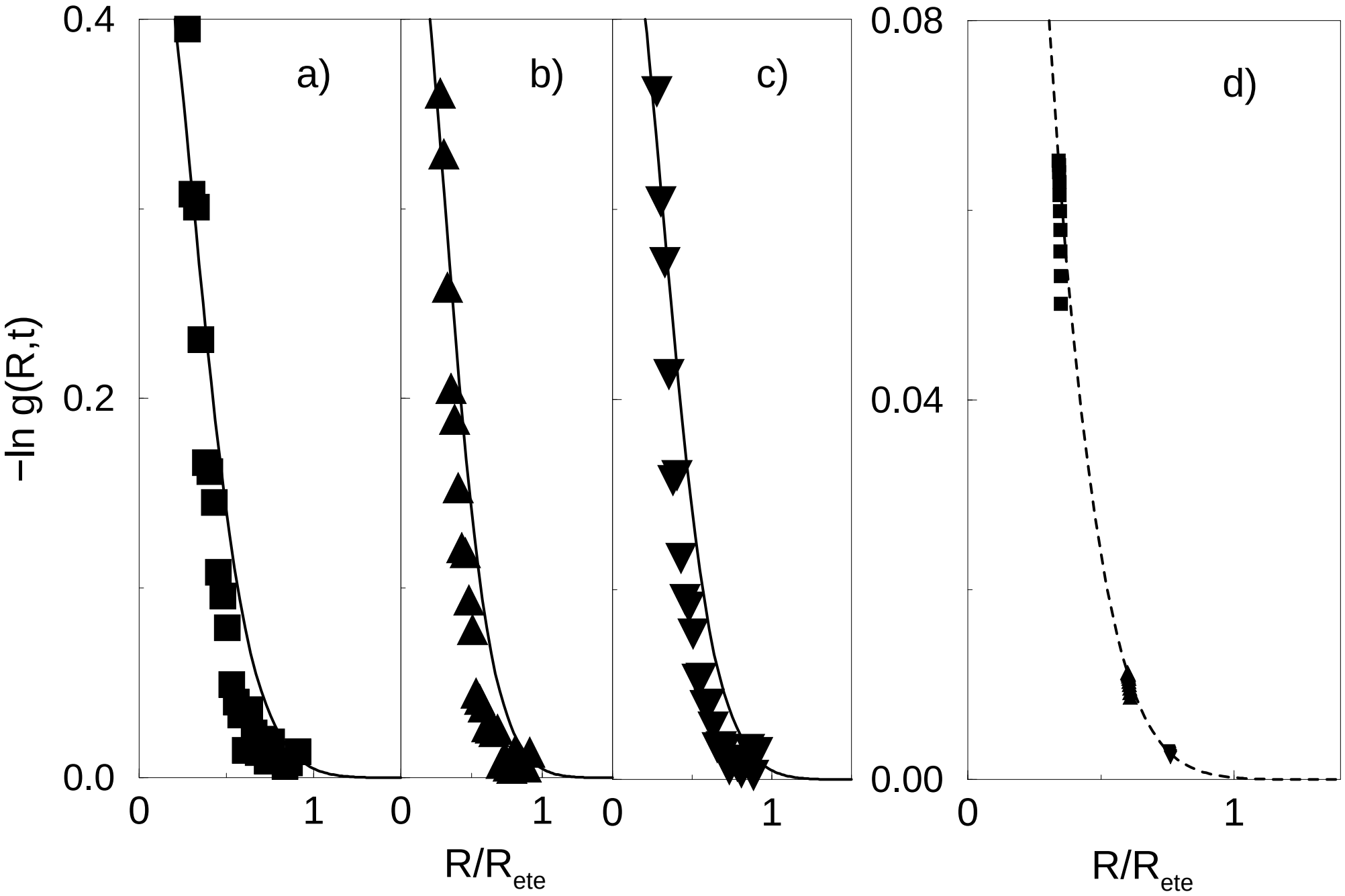
0.4
0.2
0.0
−ln g(R,t)
a)
b)
c)
d)
0
1
0
1
0
1
0.08
0.04
0.00
0
1
R/R_ete
R/R_ete

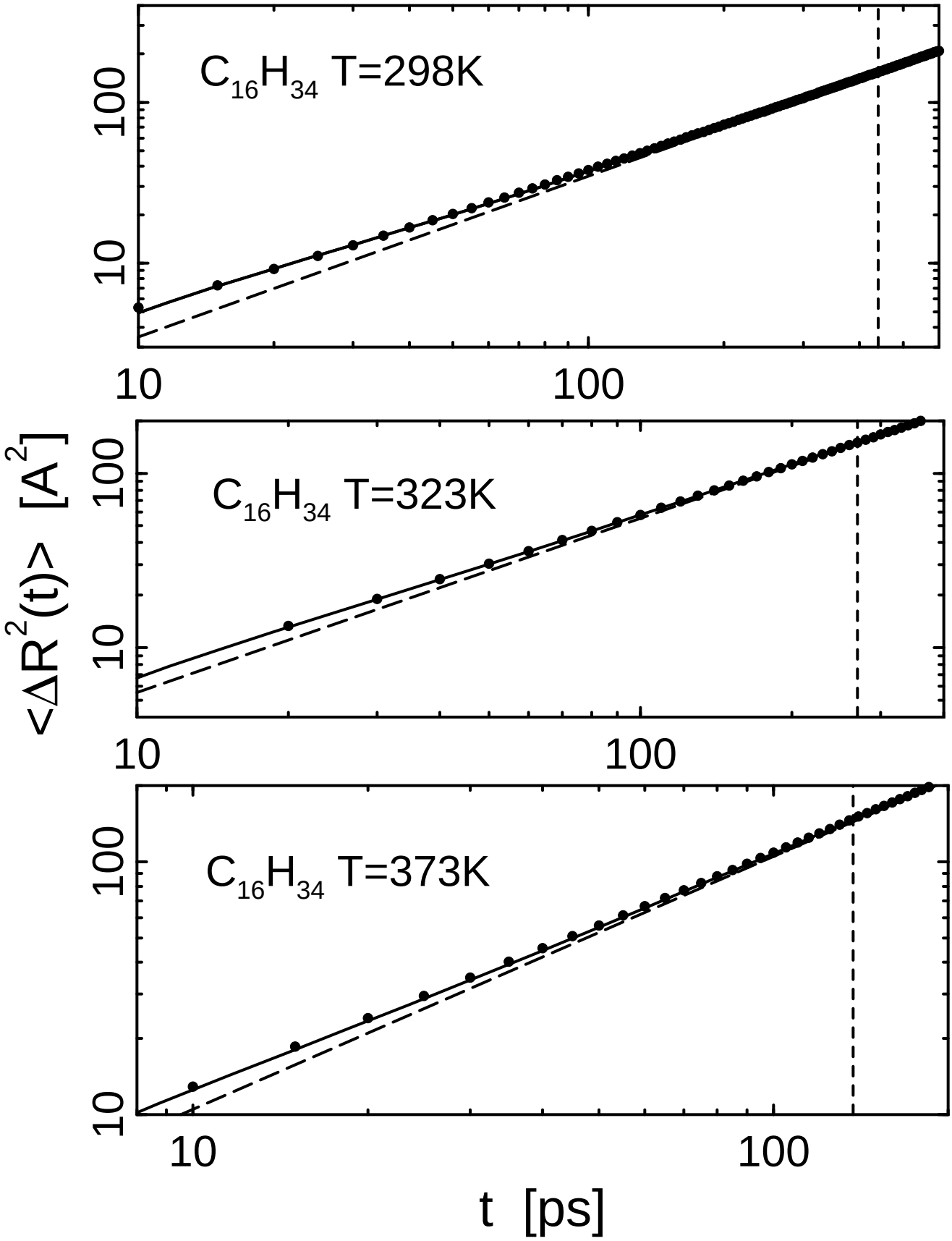

Figure 5a Guenza

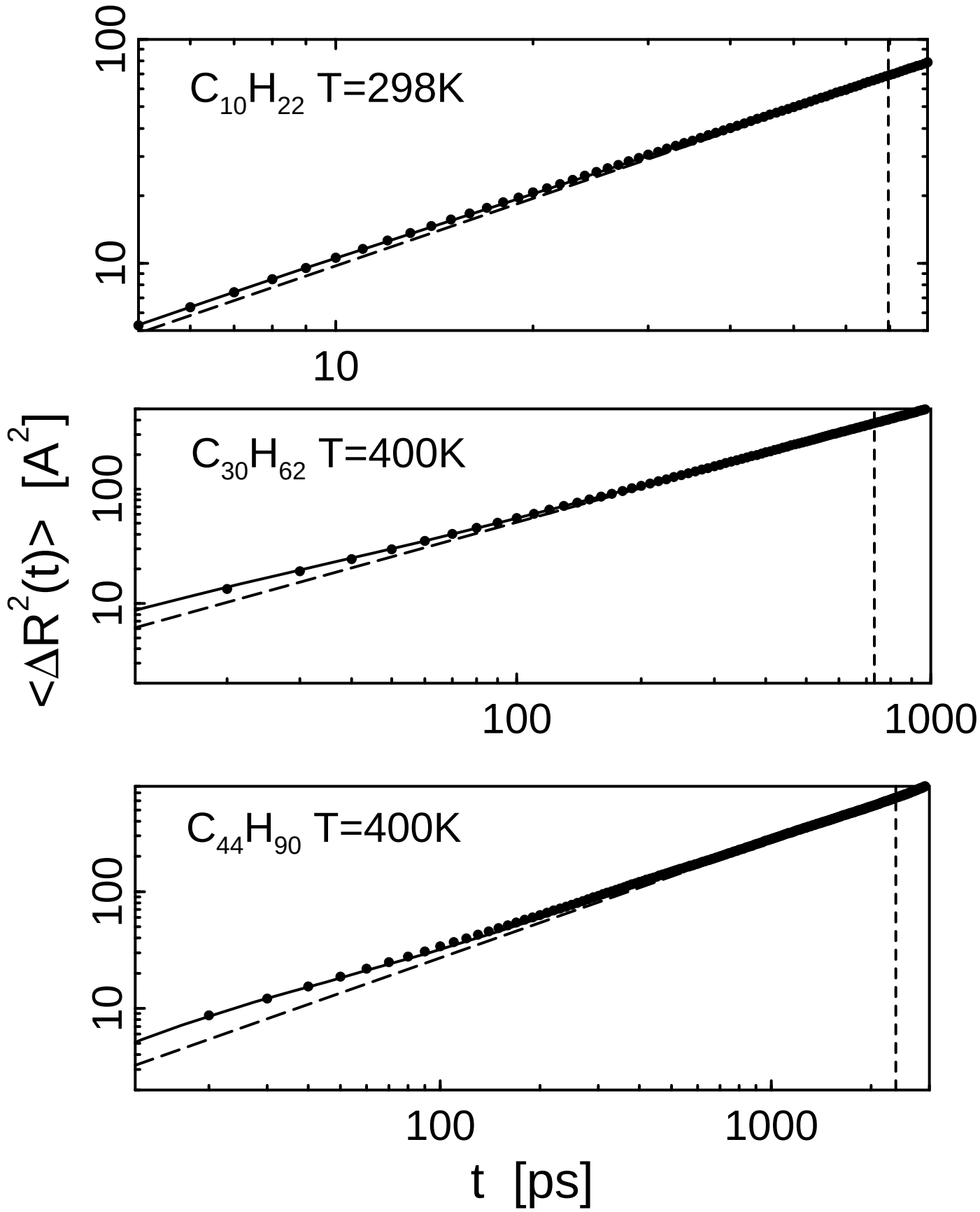

Figure 5b Guenza

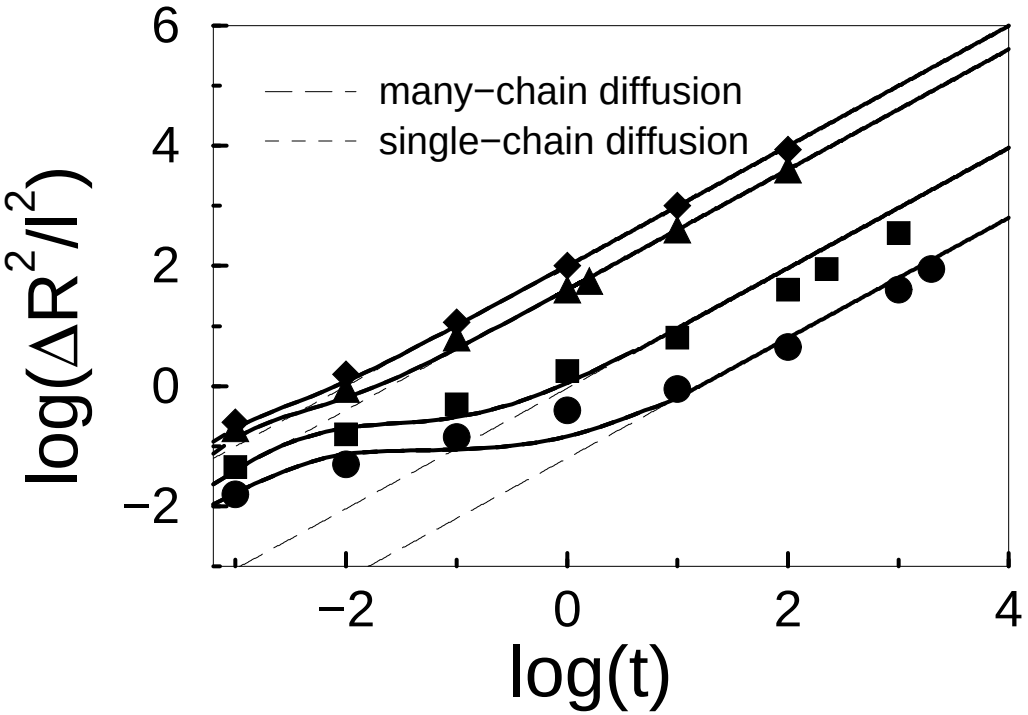

Figure 6 Guenza